Interaction of the Trojan peptide penetratin with anionic lipid membranes–a calorimetric study

Hans Binder*† and Göran Lindblom

Department of Biophysical Chemistry, Umeå University, SE-90187, Umeå, Sweden

We studied the thermodynamics of binding of the cell-penetrating peptide penetratin with mixed dioleoylphosphatidylcholine/dioleoylphoshatidylglycerol (DOPC/DOPG) unilamellar vesicles as a function of the molar fraction of anionic lipid, X_{PG}, by means of isothermal titration calorimetry. So-called lipid-to-peptide and peptide-to-lipid titration experiments were performed. The experimental data were interpreted in terms of the surface partitioning model. Membrane binding is driven by an exothermic partial molar enthalpy of $-(20–30)$ kJ mol^{-1} owing to the nonclassical hydrophobic effect and a lipid-induced change of the secondary structure of penetratin from a random coil into a more ordered α-helical and/or β-sheet conformation. The differential binding enthalpy slightly changes as a function of the content of anionic lipid in the membrane and of the molar ratio bound peptide-to-lipid. This effect presumably reflects variations of the secondary structure of bound penetratin. The small change of entropy upon binding is compatible with a superficial binding mode of the peptide with relatively small perturbations of the membrane.

Introduction

The pAntp peptide, corresponding to residues 43–58 of the homeodomain of antennapedia, also called penetratin, was the first recognized member of a rapidly expanding family of peptide-based cellular transporters originating from either natural or synthetic sources. They are also known as Trojan peptides because they are able to enter the cells presumably in an receptor-independent manner and to bring macromolecules such as small proteins, DNA,[1] and PNA oligomers into cells.[2] Also other cationic model peptides such as short oligomers of arginine or lysine enable or enhance uptake of agents into cells that do not enter or do so only poorly in unconjugated form.[3–5]

The interaction between penetratin and the phospholipid matrix of the plasma membrane seems to be an essential step involved in the translocation mechanism. Penetratin does not belong to the ampiphathic helical peptide family, whose members are able to penetrate membranes by pore formation or by a detergent-like mechanism. It was shown experimentally and by molecular modeling that penetratin is not sufficiently hydrophobic to insert deeply into the phospholipid model membranes.[6] Instead, this peptide preferentially remains at the interface between the phospholipid bilayer and the aqueous environment.

Several studies using different methods such as UV/VIS, CD and NMR spectroscopy have been carried out on penetratin in order to define the structural requirements and the mechanism of the cell penetration and to improve the carrier efficiency of the peptides.[7–15,6] Isothermal titration calorimetry (ITC) has not yet been applied to study the interaction of penetratin with lipid membranes. This calorimetric technique measures reaction heats released or consumed upon mixing of two compounds of different composition, *e.g.*, a suspension of lipid vesicles with a solution of additives such as peptides. ITC experiments are highly sensitive in detecting the binding of

peptides to lipid membranes and, in addition, provide thermodynamic information about peptide–lipid interactions (see ref. 16 for a review).

Our previous ITC study was aimed to get a better understanding of factors that affect the peptide binding to lipid membranes and its permeation through the bilayer.[17] We found that upon addition of penetratin to mixed dioleoylphosphatidylcholine/dioleoylphosphatidylglycerol (DOPC/DOPG) unilamellar vesicles the peptide first binds to the outer vesicle surface. Its binding capacity increases with the molar fraction of anionic lipid, X_{PG}. At a threshold value of $X_{PG} \approx 0.5$ and a molar ratio of bound peptide-to-lipid of $(P/L) \approx 1/20$ the membranes become permeable and penetratin binds also to the inner monolayer after internalization. Both, the cationic charge of the peptide and the anionic charge of the membrane are essential factors affecting the ability of Trojan peptides to translocate across lipid bilayers.

We interpreted our results in terms of an ''electroporation-like'' mechanism according to which the asymmetrical distribution of the peptide between the outer and inner surfaces of charged bilayers causes a transmembrane electrical field that alters the lateral and curvature stress within the membrane. At the threshold these effects induce internalization of penetratin presumably *via* inversely curved transient structures.

These results clearly indicate that electrostatics play a key role for penetratin binding and internalization. However, a charge-independent affinity of the peptide to lipid membranes may, in addition, be an important factor that affects the translocation of cargo peptides across lipid membranes. The lipid, for example, can induce a change of the secondary structure of penetratin at the membrane interface which in turn affects its hydrophobicity, and thus also its insertion mode prior to internalization. Such structural details and the thermodynamics of the interaction of penetratin with lipid bilayers remain open questions.

In this publication we adapt the surface partitioning model[18] to extract thermodynamic information about the binding and permeation process from the ITC data. In the theoretical part we analyzed the effect of model parameters such as the peptide

† Present address: Interdisciplinary Centre for Bioinformatics of Leipzig University, D-4103 Leipzig, Kreuzstr. 7b, Germany. E-mail: E-mail: binder@rz.uni-leipzig.de, fax: ++49-341-1495-119

charge and the surface charge density on the ITC heats in a systematic fashion. In the second part the experimental ITC heats are analyzed.

Materials and methods

Materials

Penetratin (Arg-Gln-Ile-Lys-Ile-Trp-Phe-Gln-Asn-Arg-Arg-Met-Lys-Trp-Lys-Lys), was solid-phase synthesized by Dr. Å. Engström at the University Uppsala (Sweden). The zwitterionic, neutral phospholipid dioleoylphosphatidylcholine (DOPC) and the anionic phospholipid dioleoylphosphatidylglycerol (DOPG) were purchased from Avanti Polar Lipids (Alabaster, AL). The lipids and the peptide were used without further purification. The experiments were carried out at 25 °C if not stated otherwise using 10 mM TRIS buffer containing 0.5 EDTA (pH 7.8) and NaCl (0.01–1 M).

Preparation of samples

Sample preparation was previously described in detail.[17] Penetratin was weighed and directly dissolved in definite amounts of buffer to give stock solutions, which were further diluted to obtain the desired sample solutions of the nominal peptide concentration. In order to reduce the problems associated with peptide adhesion of materials only glass vessels and Hamilton syringes were used for sample preparations. The final concentrations of penetratin in the samples were determined by UV absorption spectroscopy.

Stock solutions of the pure lipids DOPC and DOPG in chloroform–methanol (3:1 v/v) were mixed in definite amounts to give the desired composition of neutral and anionic lipids in terms of the molar fraction of DOPG, X_{PG}. The organic solvent was removed with a rotary evaporator and subsequently under high vacuum. The dried lipid films were re-suspended in defined buffer volumes by vortexing to give the final lipid concentration, $C_{lipid} = C_{DOPC} + C_{DOPG}$. After five freeze-thaw cycles, the lipid suspension was either passed at least 15 times through two stacked Osmonics polycarbonate membranes of 100 nm pore size in a 1 ml mini-Liposo-Fast-Pneumatic extruder (Avestin, Canada), or it was sonicated in cold water for 20 min using a titanium tip ultrasonicator followed by 10 min ultracentrifugation ($3000g$) to prepare large and small unilamellar vesicles, LUV and SUV, respectively.

Isothermal titration calorimetry

The measurements were performed using a VP isothermal titration calorimeter produced by MicroCal Inc., Northampton, MA. Data handling (baseline subtraction, peak integration, sample dilution) procedures were performed with MicroCal Origin software.

In the *lipid-to-peptide* titration (L-to-P) experiment aliquots ($\delta V_{syr} = 7$ or 10 μl) of a lipid solution ($L_{syr} = 10$–30 mM) were titrated into the sample cell of volume $V_{cell} = 1.42$ ml which initially contains the penetratin buffer solution ($P_0 = 7$–20 μM). Each injection j produces a differential heat, q_L^j (in kJ mol^{-1} of injected lipid), mainly because free peptide binds to the injected lipid. The q_L^j values decrease in (absolute) magnitude with consecutive injections because the amount of (free) peptide that binds to the vesicles progressively decreases with increasing lipid concentration (see Fig. 2 below for illustration).

Each value of q_L^j was obtained by integration over the jth heat peak measured by the ITC calorimeter after baseline subtraction. For further analysis the differential heat was corrected for a small but significant contribution mainly due to dilution effects, $\delta q_L^j = q_L^j - q_L^{dil}$. This correction was either estimated in independent blank experiments (lipid-to-buffer)

or it was set equal to the asymptotic q_L^j value reached in the L-to-P experiment at higher injection numbers. The cumulative heat of reaction after i injections,

$$Q_L^i = \sum_{j=1}^{i} \delta q_L^j, \tag{1}$$

thus provides a measure of the fraction of bound peptide

$$P_b/P \approx Q_L^i/Q_L^{tot} \tag{2}$$

where Q_L^{tot} denotes the limiting value of the cumulative heat for $i \gg 1$ and P is the peptide concentration in the calorimeter cell. Eqn. (2) assumes that only peptide binding events contribute to the observed effect and that the differential enthalpy of binding (per mol of peptide which binds) is a constant. Effectively the cumulative heat provides a mean value of the differential binding enthalpy averaged over the respective range of effective concentrations of bound peptide (see below)

$$\langle \Delta h_P^b \rangle \approx Q_L^{tot}(\delta V_{syr} L_{syr})/(V_{cell} P_0) \tag{3}$$

In the *peptide-to-lipid titration* (P-to-L) experiment aliquots of a peptide solution ($\delta V_{syr} = 7$ or 10 μl; $P_{syr} = 0.2$–0.5 mM) were titrated into the sample cell which initially contains only lipid vesicles ($L_0 = 0.2$–0.5 mM). The integral over each heat peak provides the differential heat of reaction caused by injection j, q_P^j (in kJ per mol of injected peptide). It was corrected for dilution effects according to $\delta q_P^j = q_P^j - q_P^{dil}$. The dilution heat q_P^{dil} was estimated in analogy to the L-to-P experiment (*vide supra*).

Theory

The effect of electrostatics on the observed ITC heats

The enthalpy of the aqueous peptide/lipid mixture can be written as $H = h_L N_L + h_P N_P$ where the $N_i = iV_{cell}$ ($i = L, P$) denote the moles of lipid and peptide in the calorimeter cell. The respective partial molar enthalpies are given by $h_i \equiv \partial H/\partial i = h_P^b \partial P_b/\partial i$ ($i = L, P$) with $h_P^b \equiv \partial H/\partial P_b$. The respective change of the Gibbs free energy defines the chemical transfer potential of membrane-bound peptide, $\mu_P^b \equiv \partial G/\partial P^b = h_P^b - Ts_P^b$ where s_P^b is the respective partial molar entropy of the membrane-bound peptide. Note that the differential values of peptide binding, h_P^b, s_P^b and μ_P^b refer to changes of the enthalpy, entropy and Gibbs free energy upon *transfer* of 1 mole peptide from the aqueous into the membrane phase, respectively.

The observed heat in the P-to-L (or in the L-to-P) titration experiment is given by the partial molar enthalpy, h_P (or h_L), plus the dilution heat according to

$$q_P = h_P + q_P^{dil} = \frac{\Delta P_b}{\Delta P} h_P^b + q_P^{dil}$$
$$q_L = h_L + q_P^{dil} = \frac{\Delta P_b}{\Delta L} h_P^b + q_L^{dil}, \tag{4}$$

respectively. The "deltas" of P and L denote the respective concentration changes in consecutive injections owing to addition of peptide and lipid, respectively. In the calculations we used representative concentration increments of the respective ITC experiments for ΔP and ΔL. The concentration of bound peptide is related to the total peptide and lipid concentrations, P and L, by means of a binding equilibrium according to

$$(P_b/L) = (P/L)K_{app}\gamma L/(1 + K_{app}\gamma L) \tag{5}$$

where

$$K_{app} = K_b \exp\left(-\frac{z_P F\psi_0}{RT}\right), \tag{6}$$

and K_b define the apparent and the intrinsic binding constant of penetratin, respectively. For a detailed discussion of peptide-membrane interactions in terms of binding and partitioning equilibria we refer to the review of White *et al.*[19] The surface potential of the membrane, the Faraday constant, the gas constant and the temperature are denoted by ψ_0, F, R and T, respectively. We assume that only a fraction γ of the lipid, L, is accessible to peptide binding. The peptide carries an effective charge z_P which typically differs from its nominal charge z (see below).

Differentiation of eqn. (5) with respect to the concentration of the injected compound in the L-to-P and P-to-L experiments provides the increment of bound peptide as a function of K_{app}:

$$\Delta P_b / \Delta P = \gamma L K_{app}/(1 + \gamma L K_{app})$$
$$\Delta P_b / \Delta L = (P/L)\gamma L K_{app}/(1 + \gamma L K_{app})^2. \quad (7)$$

The effective molar ratio of bound peptide to lipid in the respective leaflet of the bilayer is given by

$$(P/L)_b = P_b/(\gamma L) = (P/L)K_{app}L/(1 + K_{app}\gamma L). \quad (8)$$

The surface charge density, σ, of the DOPC/DOPG membrane with bound peptide is

$$\sigma = \frac{e}{A_L} \frac{-X_{PG}(1 - f_{Na}) + z_P(P/L)_b}{1 + (A_P/A_L)(P/L)_b}, \quad (9)$$

where e is the elementary charge, A_L the area per lipid molecule within the membrane plane, A_P and z_P the effective area and charge of the peptide, respectively, and X_{PG} denotes the molar fraction of the anionic lipid DOPG in the mixed DOPC/DOPG membrane. The fraction of DOPG associated with Na^+ was calculated according to a Langmuir isotherm, $f_{Na} = K_{Na}C_{Na}\exp(-\psi_0 F/RT)/(1 + K_{Na}C_{Na}\exp(-\psi_0 F/RT))$. Here K_{Na} is the Na^+ binding constant, taken as 0.6 M^{-1},[20] and C_{Na} is the concentration of Na^+. For the area requirement of the lipid and peptide in the membrane plane we used $A_L = 0.7$ nm^2 and $A_P = 1.5$ nm^2, respectively. The latter value was arbitrarily chosen in similarity to that of other peptides of comparable size (see, *e.g.*, ref. 18). The actual value of A_P for penetration is however unknown. Note that the choice of A_P has only a tiny effect on the calculated data at the small $(P/L)_b$ values considered here (see eqn. (9)). Also variation of A_L within 10% has virtually no effect on the results.

The surface charge density and the respective surface potential, ψ_0, are related each to another by means of the Gouy–Chapman theory (see, *e.g.*, ref. 18), $\sigma^2 = 2000\varepsilon_0\varepsilon_w RT \sum_i C_i(\exp(-z_i F\psi_0/RT) - 1)$. In the calculations we used the Grahame equation for 1:1 electrolytes

$$\psi_0 \approx -\frac{RT}{F} a\cosh\left(\frac{\sigma^2}{4000\varepsilon_0\varepsilon_w C_{Na}} + 1\right), \quad (10)$$

where ε_0 is the permittivity of vacuum and $\varepsilon_w = 81$ the dielectric constant of water. Note that eqn. (10) takes into account only monovalent ionic species and ignores the effect of free cationic peptide. The consideration of multivalent ions in the Gouy–Chapman theory results in the necessity of introducing additional parameters such as an exclusion surface and an interacting charge magnitude[21,22] which have been omitted here for sake of simplicity. This approach is justified at small peptide concentrations used in this work.

We compute heat courses for the P-to-L and L-to-P experiments by means of eqn. (4) in terms of reduced heats, $q_P^* \equiv -q_P/h_P^b$ and $q_L^* \equiv -q_L/h_P^b$, to assess the effect of the model parameters z_P, K_b and X_{PG} at $T = 25\,°C$ (Fig. 1). Dilution heats are neglected in the model calculations. In this particular case the reduced heats directly provide the respective increments of bound peptide, $q_P^* = -\Delta P_b/\Delta P$ and
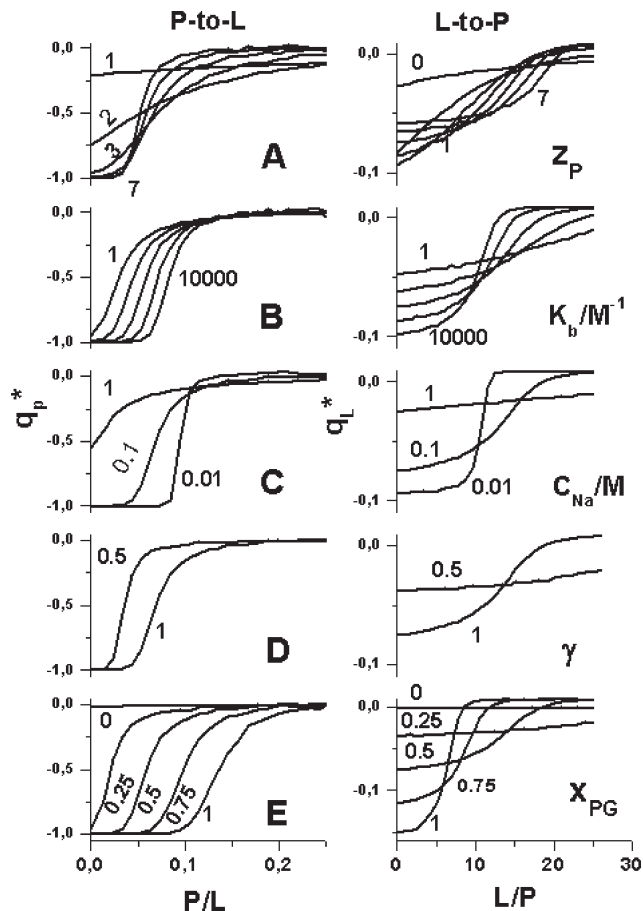
Fig. 1 Theoretical titration curves of the P-to-L (*left*) and L-to-P (*right*) ITC experiments as a function of the molar ratio peptide-to-lipid and lipid-to-peptide, respectively. The heat effect is given in terms of reduced heats $q_P^* \equiv -q_P/h_P^b$ ($P \to 0$) and $q_L^* \equiv -q_L/h_P^b$ ($L \to 0$) for the P-to-L and L-to-P experiment, respectively. The curves were calculated according to eqns. (4)–(10) making use of the standard set of parameters $z_P = 5$, $K_b = 100$ M^{-1}, $C_{Na} = 0.1$ M, $X_{PG} = 0.5$ and $\gamma = 1$. Each row of Figures corresponds to the variation of one parameter whereas the others were set equal to that of the standard set: $z_P = 1, 2, 3, 4, 5, 6, 7$ (part A) $K_b = 1, 10, 10^2, 10^3, 10^4$ M^{-1} (B) $C_{Na} = 0.01, 0.1, 1$ M (C) $\gamma = 0.5, 1.0$ (D) and $X_{PG} = 0, 0.25, 0.5, 0.75, 1$. (E) Dilution heats were neglected (eqn. (4)). The variation of the lipid and peptide concentration refers to that of ITC experiments with $P_{syr} = 0.4$ mM, $L_0 = 0.2$ mM, $\delta V_{inj} = 10$ μl for the P-to-L and $L_{syr} = 3$ mM, $P_0 = 0.025$ mM, $\delta V_{inj} = 7$ μl for the L-to-P experiment. Note that the discrete increments of ΔP and ΔL give rise to a slightly stepwise shape of the calculated curves.

$q_L^* = -\Delta P_b/\Delta L$ (see eqn. (7)). Fig. 2 depicts the concentration of free and membrane bound peptide and the surface charge density as a function of the (P/L) and (L/P) molar ratios in typical P-to-L and L-to-P experiments, respectively.

Inspection of Figs. 1 and 2 reveals the following properties:

(i) In the P-to-L experiment the injected peptide binds completely (*i.e.*, $P_b \approx P$, $q_L^* \approx 1$) at small (P/L) values ($P \to 0$) and $z_P > 3$, $C_{Na} \leq 0.1$ mM, $K_b \geq 1$ M^{-1} and $X_{PG} \geq 0.25$. This concentration range refers to strong binding because the surface charge density (and the surface potential) of the anionic lipid membrane is minimum and consequently K_{app} is maximum (see eqn. (7), $\Delta P_b(P \to 0)/\Delta P \approx 1$ for $K_{app}L \gg 1$). Consequently, the P-to-L experiment allows to estimate the differential binding heat in the limit of small peptide concentration, $h_P^b(P \to 0)$.

(ii) The limiting regime of strong binding ($K_{app}L \gg 1$) switches over into the saturation-like behavior ($K_{app}L \ll 1$) at critical conditions referring to $K_{app}L = 1$ at which 50% of injected peptide associates with the membranes ($\Delta P_b/\Delta P = -q_P^* = 0.5$). At higher peptide concentrations newly
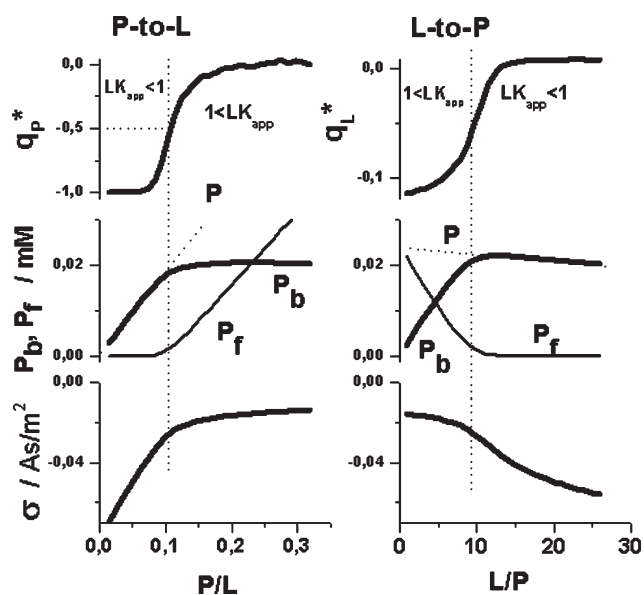
Fig. 2 Reduced reaction heats of the P-to-L and L-to-P titration experiments as a function of (P/L) and (L/P) molar ratios (upper panel), the respective concentration of total (P), bound (P_b) and free peptide (P_f) and the surface charge density $(\sigma,$ below). The curves refer to the standard set of parameters (see legend of Fig. 1).

injected peptide predominantly remains free in solution owing to saturation-like behavior $(\Delta P_b/\Delta P \ll 1)$. This behaviour can be easily detected in the ITC experiment.

(iii) Both the intrinsic binding constant, K_b (Fig. 1A), and the effective charge, z_P (Fig. 1B), affect the horizontal shift between the P-to-L curves and the slope in their rising part to a comparable extent. A joint analysis to determine K_b and z_P from one q_P curve appears not reasonable.

(iv) The variation of the considered parameters mainly causes a horizontal shift of the P-to-L curves each to another along the (P/L)-concentration axis. The strongest effect is induced by alteration of the molar fraction of anionic lipid in the membrane (Fig. 1E). Hence, a series of P-to-L experiments with different X_{PG} represents the optimal setup to determine the effective charge of the peptide.[17]

(v) The L-to-P experiments show analogous properties as the P-to-L experiments. The values of the observed heats of the first injections however considerably vary as a function of the model parameters. In the limit of small lipid concentrations eqn. (7) provides $\Delta P_b(L \to 0)/\Delta L \approx P\gamma K_{app}$ $(K_{app}L \ll 1)$. Hence, the increment of bound peptide in the first injections and thus the observed heat is directly related to the apparent binding constant and the accessibility factor (eqn. (4)).

The differential binding enthalpy is not necessarily a constant. In general, it represents a function of the effective concentration of bound peptide in the membrane, $(P/L)_b$ (see also the Discussion section below). The L-to-P titration thus provides an estimation of h_P^b in the limit of small lipid concentration, $h_P^b(L \to 0)$, i.e. at high values of $(P/L)_b$, whereas the P-to-L experiment yields an estimation of h_P^b in the limit of small peptide concentration $h_P^b(P \to 0)$, i.e. at small values of $(P/L)_b$. Comparison of the differential binding enthalpy in the limit of small and high $(P/L)_b$, $h_P^b(P \to 0)$ and $h_P^b(L \to 0)$, respectively, with its mean value, $\langle \Delta h_P^b \rangle$ (eqn. (3)), allows to prove the assumption of constant differential binding enthalpy.

Experimental results

Lipid-to-peptide titration experiments

Fig. 3 shows the results of a typical L-to-P titration experiment. Integration of the exothermic heat pulses recorded after
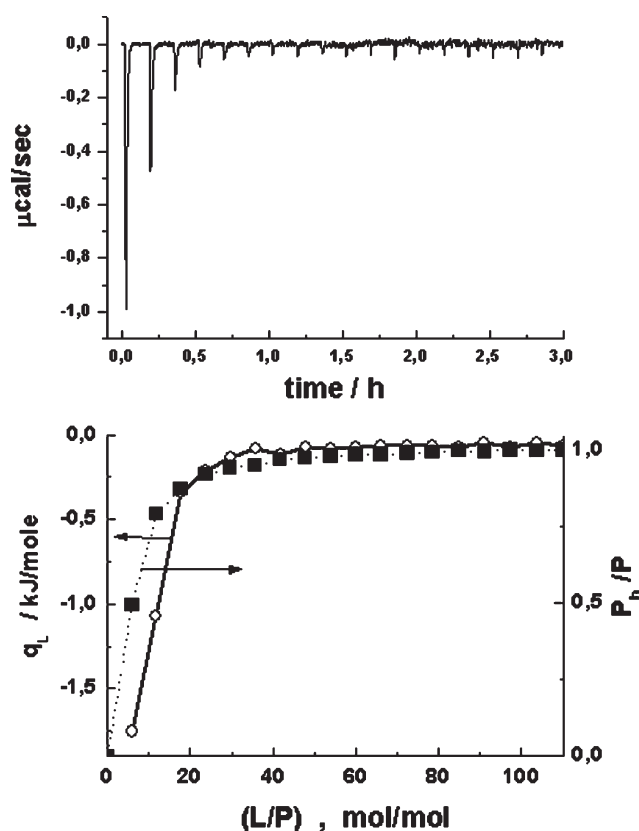

Fig. 3 Lipid-to-peptide titration experiment: aliquots $(\delta V_{syr} = 7 \ \mu l)$ of a lipid suspension $(L_{syr} = 15$ mM, DOPC/DOPG SUV, $X_{PG} = 0.75$, TRIS + 100 mM NaCl) were titrated into a penetratin solution $(P_0 = 0.0125$ M, same buffer). The top panel shows the calorimeter tracings. The bottom panel shows the differential (open symbols, left ordinate) and the fraction of bound peptide (solid symbols, right ordinate, cf. eqn. (2)) as a function of the molar ratio lipid-to-peptide in the sample cell.

each injection yields the differential reaction heat, q_L, in units of kJ mol^{-1} of injectant. The released heat results from the binding reaction of a certain amount of penetratin with the injected lipid. After each injection, the concentration of free, available peptide decreases owing to progressive membrane binding (see also Fig. 2). Consequently, the absolute value of the differential heat continuously decreases with increasing injection number, since less penetratin binds to the vesicles in consecutive injections. After 4–5 injections almost all peptide is bound and further addition of lipid entails no further reaction. The remaining small differential heat can be mainly attributed to dilution effects. After correction one obtains the cumulative heat of reaction (see Fig. 3 and eqn. (1)) the asymptotic value of which provides a measure of the mean differential heat of peptide binding $\langle h_P^b \rangle \approx 21$ kJ mol^{-1} (eqn. (3) and Table 1).

Fig. 4 shows a series of L-to-P titration experiments with mixed DOPC/DOPG vesicles containing a variable fraction of anionic DOPG, X_{PG}. Penetratin, formally carrying seven positive charges, interacts with negatively charged membranes via Coulombic forces. An increasing fraction of anionic DOPG in the bilayer decreases the (negative) surface charge density of the membranes and thus their affinity for penetratin binding. The absolute value of the differential heat, $q_L(L \to 0)$, of the first injections increases with increasing molar fraction of anionic DOPG, X_{PG} whereas the number of injections that are necessary to bind the dissolved peptide decreases (Fig. 4). Theory predicts $|q_L(L \to 0)| \propto K_{app}$ (vide supra), and thus an increasing absolute value of $q_L(L \to 0)$ with decreasing (negative) surface potential (see eqn. (6)) in agreement with the observation.

Table 1 Binding parameters of penetratin to DOPC/DOPG membranes

X_{PG}	K_{app}/K_b [a]	$\mu_P^{app}/$ kJ mol^{-1} [b]	$h_P^b(P\to0)/$ kJ mol^{-1} [c]	$Ts_P^b(P\to0)/$ kJ mol^{-1} [d]	$h_P^b(L\to0)/$ kJ mol^{-1} [e]	$\langle h_P^b\rangle/$ kJ mol^{-1} [f]	X_{helix} (%) [g]
0.0	1	−21	−18 ± 3	+3 ± 5	–	–	21
0.25	2 × 10^5	−34	−33 ± 5	−13 ± 6	−18 ± 4	−25 ± 4	63
0.5	4 × 10^5	−36	−23 ± 4	−3 ± 6	−18 ± 4	−20 ± 4	53
0.75	2 × 10^{11}	−68	−21 ± 4	−1 ± 6	−11 ± 4	−21 ± 4	30
1.0	4 × 10^{11}	−70	−17 ± 2	+3 ± 4	−14 ± 3	−16 ± 3	31

[a] Calculated according to eqn. (6) using an intrinsic binding constant $K_b = 80$ M^{-1} taken from ref. 10. [b] Calculated according to $\mu_P^{app} \equiv (\partial G/\partial P)^{surface} = -RT\ln(55.5K_{app}) = \mu_P^b + z_PF\psi_0(P\to0)$ where the chemical transfer potential of peptide upon binding is $\mu_P^b \equiv \partial G/\partial P^b = -RT\ln(55.5K_b) = -21$ kJ mol^{-1}. The electrostatic potential refers to $P\to0$. [c] Obtained by means of $h_P^b(P\to0) \approx q_P - q_P^{dil}$, where q_P and q_P^{dil} are the respective differential reaction heat of the P-to-L experiment and the respective dilution heat. [d] Partial molar transfer entropy of the peptide upon binding $Ts_P^b \equiv T\partial S/\partial P_b = h_P^b - \mu_P^b$. [e] Obtained by fits of eqn. (4) to the q_L traces of the respective L-to-P experiments. [f] Obtained from the cumulative heats of the L-to-P experiments (eqn. (3)). [g] Fraction of penetratin in the helical conformation in the presence of POPC/POPG mixed membranes containing a POPG fraction of X_{PG}. Data were taken from ref. 14.

Further indications of a charge dependent binding mode were obtained in experiments with different amounts of NaCl in the buffer solution (not shown, see ref. 17). As expected the respective absolute $q_L(L\to0)$ values decrease with increasing salt concentration owing to reduced electrostatic interactions.

Temperature dependent studies

L-to-P titration experiments with vesicles of a molar fraction of DOPG of $X_{PG} = 0.25$ were performed at $T = 15, 25, 35$ and 45 °C. No significant effect of temperature on the ITC results was observed (not shown).

Peptide-to-lipid titration experiments

Fig. 5 shows the differential reaction heats, q_P, for the titration of DOPC/DOPG vesicles with penetratin. The molar fraction of DOPG in the vesicles was varied between $X_{PG} = 0$ and 1. The heat effect observed upon titration with penetratin to neutral DOPC ($X_{PG} = 0$) is much weaker than for anionic membranes ($X_{PG} > 0$). This result confirms the charge dependent interaction of penetratin with the membranes stated above. The decreasing absolute value of q_P with increasing peptide content for $X_{PG} \leq 0.5$ reflects the fact that with each titration less of the injected peptide binds to the vesicles because the
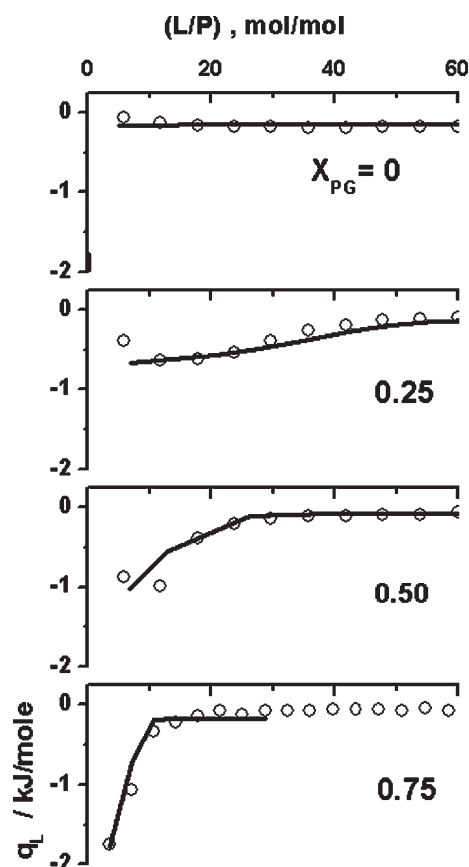
Fig. 4 Differential reaction heats of lipid-to-peptide experiments for mixed DOPC/DOPG SUV of different composition as a function of the molar ratio lipid-to-peptide in the sample cell and theoretical curves which were calculated by means of eqn. (4) with $K_b = 80$ M^{-1}, $z_P = 5.1$, $C_{Na} = 0.1$ M, $q_L^{dil} = 0.05$–0.1 kJ mol^{-1} and $\gamma = 0.5$ ($X_{PG} \leq 0.5$) and $\gamma = 1$ ($X_{PG} > 0.5$). The mole fraction of DOPG, X_{PG}, is given in the figure. Further experimental parameters are: $\delta V_{syr} = 7$ μl, SUV in TRIS + 100 mM NaCl; $L_{syr} = 15$ mM, $P_0 = 0.125$ mM.
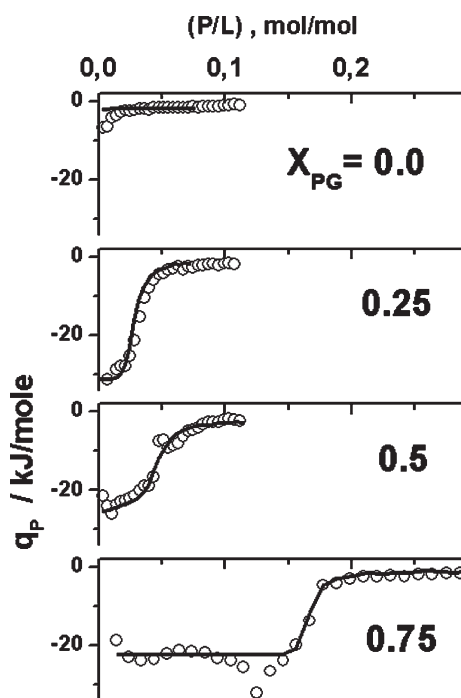
Fig. 5 Differential reaction heat of peptide-to-lipid titration experiments of penetratin into mixed DOPC/DOPG LUV of different mole fraction of DOPG, X_{PG} (see figure) as a function of the molar ratio peptide-to-lipid, (P/L), in the sample cell.. Aliquots (δV_{syr}) of penetratin solution (P_{syr}, TRIS) were titrated into a lipid dispersion. The experimental conditions are $P_{syr} = 0.2$ mM, $L_0 = 0.4$ mM, $\delta V_{syr} = 10$ μl ($X_{PG} = 0, 0.25, 0.5$) $P_{syr} = 0.4$ mM, $L_0 = 0.2$ mM, $\delta V_{syr} = 7$ μl ($X_{PG} = 0.75$). The theoretical curves were calculated by means of eqn. (4) with $K_b = 80$ M^{-1}, $z_P = 5.1$, $C_{Na} = 0.01$ M and $\gamma = 0.5$ ($X_{PG} \leq 0.5$) or $\gamma = 1$ ($X_{PG} > 0.5$).

positive charges of bound penetratin hamper further binding of the peptide, and thus effectively reduce the apparent binding constant, K_{app}. At higher injection numbers the membrane surface saturates with penetratin and no reaction heats exceeding dilution effects were measured.

Repeated P-to-L experiments that were performed at different time- and concentration scales indicate that q_P depends only on the molar ratio peptide-to-lipid, (P/L), and not on the total lipid concentration (Fig. 6). This result suggests that samples behave identically in the considered time-window ranging from several tens of minutes to several hours. Consequently, kinetic effects such as the binding of penetratin to the membrane surfaces and/or its permeation through the bilayers proceed with characteristic times which are either considerably smaller or considerably longer than the time window of the experiments.

The q_P vs. (P/L) curves exhibit a more structured course for $X_{PG} \geq 0.5$ than for $X_{PG} < 0.5$. The differential reaction heat first increases, then it turns to decrease before its absolute value drops to values near zero. The local minimum of $|q_P|$ has been interpreted as a signature of the internalization threshold at which the peptide starts to permeate the bilayer and this way binds to the inner surface of the vesicles (vide infra and ref. 17).

Theoretical titration curves

We calculated theoretical titration heats by means of eqn. (4) and the surface partition model (see Theory section). The lipid and peptide concentrations in the sample cell, their increment with injection number and the electrolyte concentration, C_{NaCl}, were taken from the respective ITC experiment. For the intrinsic binding constant and the effective peptide charge we used $K_b = 80$ M^{-1},[10] and $z_P = 5.1$,[17] respectively. The
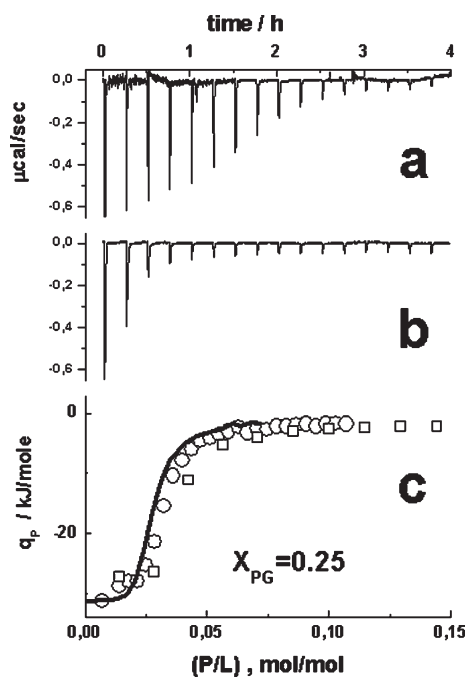
Fig. 6 Peptide-to-lipid titration experiment of penetratin to lipid LUV ($X_{PG} = 0.25$). The calorimeter traces in (a) and (b) were obtained with $P_{syr} = 0.4$ mM/$L_0 = 0.2$ mM and $P_{syr} = 0.2$ mM/$L_0 = 0.4$ mM, respectively. Because of the smaller lipid concentration in the syringe, four times more injections, and a longer time span are necessary in the first experiment to adjust a certain peptide-to-lipid molar ratio, (P/L), in the calorimeter cell. (c) Shows the differential heat of reaction as a function of (P/L). The circles and squares refer to the traces shown in (a) and (b), respectively. The thick solid curve was calculated by means of eqn. (4) with $K_b = 80$ M^{-1}, $z_P = 5.1$, $X_{PG} = 0.25$, $C_{Na} = 0.01$ M and $\gamma = 0.5$.

accessibility factor was $\gamma = 0.5$ at $X_{PG} \leq 0.5$ and $\gamma = 1$ otherwise (see ref. 17 and Discussion section). The differential binding enthalpy and the dilution heats are chosen to provide reasonable fits of the experimental data (see Figs. 4–6). The theoretical curves well reproduce the observed sigmoidal decrease of the exothermic reaction heat. Endothermic deviations of the calculated data from the experimental ones, especially in the concentration range which precedes the inflection point were discussed below.

Discussion

Penetratin binding is driven by enthalpy

Table 1 lists the differential enthalpy of penetratin binding to mixed DOPC/DOPG membranes, the respective chemical transfer potential and the differential binding entropy as a function of the molar fraction of DOPG, X_{PG}. The value of the chemical potential upon transfer of pentratin from the aqueous into the membrane phase was calculated according to $\mu_P^b = -RT\ln(WK_b) \approx -21$ kJ mol^{-1} using the intrinsic binding constant, $K_b \approx 80$ M^{-1}.[10] $W = 55.5$ M is the concentration of water in diluted solutions. Fluorescence studies of penetratin binding to mixed POPC/POPG mixed membranes of different composition indicate that K_b is virtually indepent of the lipid composition, X_{PG}.[10]

Note that the intrinsic binding constant of penetratin is slightly bigger compared with the binding constant of divalent metal cations to lipid membranes (~ 10 M^{-1},[23]), similar compared with weakly hydrophobic peptides such as magainin 2 amide ($K_b = 50$ M^{-1}),[24] SMS 201-995 (70 M^{-1}),[25] but considerably smaller than the respective binding constant of more hydrophobic peptides such as PGLa and especially melittin ($K_b = 1 \times 10^3$ M^{-1},[26] and $K_b = 4.5 \times 10^4$ M^{-1},[18] respectively). The relatively small value of the binding constant suggests that penetratin does not insert deeply into the hydrophobic core of the bilayer, but it remains superficially bound.

The chemical transfer potential provides a measure of the thermodynamic gain upon peptide binding to the membrane. It refers to "chemical" contributions owing, e.g., to the hydrophobic effect, conformational changes and/or self-aggregation of the peptide, specific peptide–lipid interactions such as H-bond formation and salt bridges and alterations of the molecular ordering within the lipid matrix (vide infra). Note that μ_P^b does not consider electrostatic effects which give rise to the enrichment of the cationic peptide near the surface of anionic membranes. In analogy to the apparent binding constant one can define an "apparent" chemical transfer potential, $\mu_P^{app} = RT\ln(WK_{app}) \approx \mu_P^b + z_P F\psi_0$, where the second term provides the respective electrostatic free energy which causes the concentration gradient of charged species near the membrane (see also Table 1).

The electrostatic contribution progressively increases with increasing content of anionic lipid in the membrane and exceeds μ_P^b at $X_{PG} > 0.5$ (Table 1). It was established in systematic binding studies of model peptides that the electrostatic contribution is a linear function rather of the effective charge of the peptide, z_P, than its formal charge, z (see Table 1 and ref. 27). As noticed above, the effective peptide valence of penetratin ($z_P \approx +5.1$) is smaller than its formal valence of $z = +7$. According to the rule-of-thumb established by Ladokhin and White, the effective valence is reduced relative to the formal valence by about 20% for each 12.5 kJ mol^{-1} of μ_P^b.[27] This rule predicts for $\Delta\mu_P^b \approx -20$ kJ mol^{-1} a reduction of the formal valence of penetratin by -2.2 to $z_P = 4.8$, which is in agreement with our estimation.

The enthalpic contribution to μ_P^b, $h_P^b (P \rightarrow 0)$, was obtained from the P-to-L titration experiments which directly provide the differential binding enthalpy of penetratin at small (P/L)

values. The injected peptide binds almost completely to the vesicles at these conditions (*vide supra*). The absolute value of the differential binding enthalpy markedly exceeds the respective entropic contribution indicating that the binding process is predominantly driven by enthalpy. The differential binding enthalpy of penetratin is however much less exothermic compared with that of amphipatic peptides such as magainin ($h_P^b < -50$ kJ mol^{-1} [28,24]) and PGLa ($h_P^b < -40$ kJ mol^{-1} [26]).

At least three effects are potentially involved into peptide binding to lipid membranes: the classical hydrophobic effect, the so-called non-classical hydrophobic effect[28] and lipid-induced conformational changes of the peptide such as the coil–helix transition. The classical hydrophobic effect, *i.e.* the release of water from the peptide upon membrane incorporation, is essentially entropy-driven at room temperature.[29] The relatively small absolute values of the differential binding entropy imply that the hydrophobic effect is not the dominating contribution of penetratin binding. This conclusion is confirmed by the ITC measurements at different temperatures. Typically, the hydrophobic effect is sensitive to changes of the temperature,[30] and thus one expects marked alterations of the binding parameters in contrast to our results.

The non-classical hydrophobic effect is characterized by an exothermic binding heat owing to favorable lipid–peptide and/or lipid–lipid interactions. Recent surface plasmon resonance and impedance measurements suggest that penetratin binding to anioinic membranes partly dehydrates their polar region, alters the conformation of the lipid headgroups and increases the lipid packing density.[11] Especially, the latter effect is expected to produce an exothermic heat of reaction. Analogous investigations on bilayers of zwitterionic phosphatidylcholines showed that the binding of penetratin is paralleled by a slight decrease in the molecular ordering of the lipid.[11] This tendency is compatible with the less exothermic values of h_P^b for pure DOPC membranes compared with the respective differential binding enthalpy for charged ones (Table 1).

Membrane binding of peptides may be enthalpically facilitated by the simultaneous transition from a random coil into an ordered α-helical and/or β-sheet conformation.[31] Spectroscopic studies indeed report indications that penetratin adopts an α helical and/or β-sheet structure at membrane surfaces[14,9,32,33] in contrast to its predominantly random coil conformation in aqueous solution.[9,14,6,34,12] Helix formation entails an enthalpy gain of about -2.9 kJ mol^{-1} per residue.[25] Using this value one expects a coil $\rightarrow$ helix transition enthalpy of about -45 kJ mol^{-1} for the 16 residues of penetratin. The measured $h_P^b (P \rightarrow 0)$ values amounts to 40–70% of this value (Table 1). This crude estimation shows that the membrane-induced conformational transition of penetratin is expected to produce an exothermic enthalpic contribution which is comparable with the observed reaction heat (see also next paragraph).

The effect of lipid composition on the binding enthalpy

The CD spectrum of penetratin in the presence of mixed POPC/POPG vesicles shows a mixture of α-helical, β-sheet and random coil conformational states in the limit of low peptide concentration ((P/L) = 0.008).[14] The fraction of helical penetratin reaches a maximum ($X_{helix} \approx 0.6$) at a content of the anionic lipid in the membranes of $X_{PG} \approx 0.2$–0.3. Interestingly, our ITC experiments reveal the maximum exothermic differential binding enthalpy, $h_P^b (P \rightarrow 0) \approx -30$ kJ mol^{-1}, at a similar molar fraction of anionic DOPG (see Table 1). The observed variation of $h_P^b (P \rightarrow 0)$ with X_{PG} possibly reflects subtle changes of the peptide conformation as a function of the surface charge density of the membrane. This interpretation is further supported by the decrease of $h_P^b (P \rightarrow 0)$ and of the helical fraction at $X_{PG} > 0.3$.[14] The spectral analysis shows

that the lowering of X_{helix} is accompanied by a concurrent increase of the β-sheet content of penetratin.[14] The differential binding enthalpy $h_P^b (P \rightarrow 0)$ varies by about $+10$ kJ mol^{-1} in the respective concentration range. This value gives rise to a hypothetical transition enthalpy between α-helical and a β-sheet conformations of $\Delta h_P(\alpha \rightarrow \beta) \approx +35$ kJ mol^{-1} if one takes into account that only 30% of the peptide effectively transforms into a β structure according to the data of Magzoub *et al.*[14]

The effect of penetratin concentration on the binding enthalpy

Inspection of the heat traces of the P-to-L experiments for $X_{PG} \geq 0.25$ reveals a continuous decrease of the absolute value of the reaction heat with increasing injection number in the (P/L) range which precedes the sigmoidal change of q_P. This tendency gives rise to a systematic deviation between the measured and calculated reaction heats. Note that the latter values are virtually constant at small (P/L) molar ratios (see Fig. 5). The observed change of the reaction heat can be rationalized if one assumes that the intrinsic binding constant and/or the differential binding enthalpy are functions of the effective concentration of membrane bound penetratin, $(P/L)_b$, which is increases with the total molar ratio (P/L) (see eqn. (8)). The former option ($K_b =$ var.) can be rejected as the main reason for the observed effect because a variation of the intrinsic binding constant over several orders of magnitude does virtually not affect the initial values of the differential binding heat (see Fig. 1B).

We therefore suggest that the absolute value of the differential binding enthalpy, h_P^b, decreases as a function of the effective peptide content in the membrane, $(P/L)_b$. Two additional observations confirm this hypothesis. At first, the cumulative reaction heat of the L-to-P experiments provides the mean exothermic differential binding enthalpy, $\langle \Delta h_P^b \rangle$, averaged over the ($L/P$) range (eqn. (3)). The $\langle \Delta h_P^b \rangle$ values are slightly but systematically smaller than the $\Delta h_P^b (P \rightarrow 0)$ data of the P-to-L experiments. Secondly, also the $\Delta h_P^b (L \rightarrow 0)$ values, which were used to fit the q_L courses of the L-to-P titrations by means of eqn. (4), are smaller in absolute magnitude than the respective $\Delta h_P^b (P \rightarrow 0)$ data. Since the L-to-P and P-to-L experiments start at high and at low (P/L) ratios, respectively, they are expected to provide different reaction heats according to the sequence $\Delta h_P^b (P \rightarrow 0) < \langle \Delta h_P^b \rangle < \Delta h_P^b (L \rightarrow 0)$ in agreement with our results.

Hitherto the calculations according to eqn. (4) assume a concentration-independent differential binding enthalpy referring to the limit of a small peptide content, $\Delta h_P^b (P \rightarrow 0)$ for the P-to-L titrations. For the sake of simplicity let us now assume that the differential binding enthalpy represents a linear function of the effective molar ratio of bound peptide in the membrane, $(P/L)_b = P_b/\gamma L \approx P/\gamma L$,

$$h_P^b = h_P^b (P \rightarrow 0)\{1 - k(P/\gamma L)\}. \quad (11)$$

The experimental data provide $k = 3.0 \pm 0.5$ under the assumption that penetratin initially binds only to the outer monolayer of the lipid vesicles at (P/L) < 0.05 ($\gamma = 0.5$, *vide infra*).

CD dichroism spectroscopy indicates an increasing fraction of penetratin in the β-sheet conformation at the expense of α helical peptide upon binding to mixed POPC/POPG membranes with increasing (P/L) molar ratio.[14] According to these measurements the helical fraction decreases by 10–20% if, for example, (P/L) increases from 0 to 0.03. From the change of the reaction heat with X_{PG} we estimated a value of the respective differential transition enthalpy of $h_P(\alpha \rightarrow \beta) \approx 20$–50 kJ mol^{-1} if one attributes the enthalpic effect exclusively to the change of secondary structure. This estimation roughly agrees with the respective value which

was obtained from the variation of the differential binding enthalpy with X_{PG} (*vide supra*).

In addition to changes of the secondary structure also other effects such as intermolecular peptide–peptide interactions and the classical hydrophobic effect potentially contribute to the observed alteration of the differential binding enthalpy. The net effect is enthalpically unfavorable and thus it must be driven by entropy.

The enthalpic effect of internalization

The reaction heat of the P-to-L experiment varies in a complex fashion at molar fractions of the anionic lipid, $X_{PG} \geq 0.5$. We recently interpreted this behavior in terms of four characteristic concentration ranges.[17] In the concentration range I, $0 \leq (P/L) < (P/L)_{threshold}$, the peptide is unable to translocate the bilayers, and thus it binds exclusively to the outer surface of the vesicles (see Fig. 7). The asymmetrical distribution of the peptide between the outer and inner surfaces of the charged bilayer causes a transmembrane electrical field that alters the lateral and curvature stress acting within the membrane by means of so-called Maxwell stresses and/or asymmetrical electrostatic dilation. Both effects are thought to reduce the stability of the bilayer.

At a certain fraction of bound peptide the electric field reaches a critical threshold value followed by an "electroporation-like" permeabilization of the membrane. Further binding of peptide destabilizes the membrane and induces its internalization. Hence, in the respective concentration range II, $(P/L)_{threshold} \leq (P/L) < (P/L)_{II}$, a certain fraction of the peptide permeates the membranes and binds to the inner leaflet of the bilayers. Note that the surface charge of the anionic lipid in the outer leaflet of the vesicle bilayers is mainly compensated by bound cationic peptide at the threshold. A similar result was recently obtained for polylysine interacting with anionic vesicles.[35] Maximum permeability of the vesicle membranes was found when 50–100% of lipid charges are neutralized by polylysine.

In range III, $(P/L)_{II} \leq (P/L) < (P/L)_{III}$, the exothermic reaction heat markedly drops because the increasing amount of bound peptide progressively compensates the anionic surface charge of the membranes. As a consequence, the membrane effectively saturates for penetratin binding and finally the reaction heat virtually vanishes in the saturation range IV, $(P/L)_{III} \leq (P/L)$.

The initial decrease of the exothermic reaction heat, q_p, in range I is followed by the moderate increase in the absolute value of q_P in range II (see Fig. 7). Such behavior was interpreted in terms of the internalization threshold when currently injected peptide induces the translocation of penetratin from the outer to the inner monolayer of the vesicle bilayers. The translocation of peptide through the membrane decreases the effective concentration of bound peptide because permeation enables distribution of penetratin between both leaflets of the bilayer (see also ref. 36). The decrease of the effective concentration of bound peptide after internalization is, in turn, paralleled by an increased absolute value of the differential binding enthalpy, and thus with the increase of the exothermic reaction heat. Note that the change of the reaction heat at the internalization threshold is a direct consequence of the monotoneous variation of the differential binding enthalpy as a function of the effective concentration of bound penetratin (see, *e.g.*, eqn. (11)).

Note that models describing composition-dependent enthalpies of additives which bind either exclusively to the outer half or equally to both halves of the bilayers are not able to explain the local minimum of the absolute value of the reaction heat.[37] Alternatively one could assume a reverse $\beta \rightarrow \alpha \rightarrow$ coil transformation of the secondary structure of penetratin with increasing concentration of bound peptide but such tendency was not observed in the respective CD spectra.[14,9]

Formally one can suggest two simple scenarios of penetratin internalization:

(A) At the threshold the additive equally distributes between both halves of the bilayer. Hence, suddenly all the lipid becomes accessible for all peptide at $(P/L) = (P/L)_{threshold}$.[36] The system switches from an enthalpic state corresponding to, *e.g.*, $\gamma_I = 0.5$ into that of $\gamma_{II} = 1.0$ resulting in two consequences for the differential reaction heat. First, the difference between the cumulative heats of both states, $\Delta Q = Q(\gamma = 1) - Q(\gamma = 0.5)$, which accumulates in range I up to $(P/L)_{threshold}$ abruptly releases upon internalization giving rise to an exothermic heat peak. Second, the reaction heat follows the curve for $\gamma = 1$ with further increasing peptide concentration in ranges II, III and IV (see the dotted line in Fig. 7).

(B) Only a certain amount of the additive exceeding the threshold value $(P/L)_{threshold}$ permeates the bilayer and binds to the inner vesicle surface. The peptide-to-lipid molar ratio of the outer surface remains constant in range II whereas the peptide concentration at the inner surface increases. The resulting reaction enthalpy switches from the line for, *e.g.*, $\gamma_I = 0.5$ to a similar line which is however shifted by $(P/L)_{threshold}$ along the concentration axis.

Heat traces according to scenarios A and B were shown in Fig. 7 for $X_{PG} = 0.50$ and 0.75 together with the respective experimental data. The sudden equilibration of the peptide between the inner and outer vesicle surfaces at the internalization threshold as suggested for scenario A gives rise to a sharp exothermic peak and a downwards step of the reaction heat. Scenario B causes only a step in the q_P course. Although the considered scenarios should be viewed as a not quite realistic, limiting cases, the experimental data indicate some qualitative agreement with the calculated curves. The measured data can, for example, be interpreted in terms of a "mixture" of both scenarios A and B if one assumes that the exothermic peak "smears" over a number of subsequent injections, since the internalization threshold does not reflect total equilibration, but only the onset of a gradual internalization process. Possibly, only penetratin molecules exceeding a certain local threshold concentration of bound

(P/L) , mol/mol
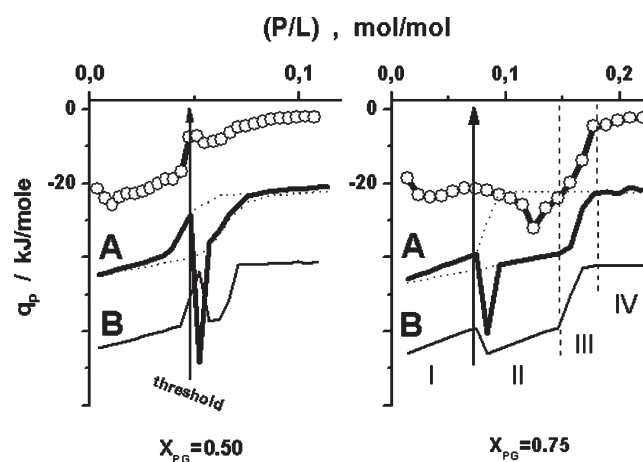
Fig. 7 Differential heats of P-to-L titration experiments with DOPC/DOPG vesicles containing a DOPG mole fraction of $X_{PG} = 0.5$ (left) and 0.75 (right). The symbols are experimental data (see legend of Fig. 5 for details). The curves below were calculated by means of eqns. (4)–(10). The dotted curves correspond to a constant accessibility factor $\gamma_I = 0.5$ and $\gamma_{II} = 0.7$ for $X_{PG} = 0.5$ and $\gamma_I = 0.5$ and $\gamma_{II} = 1$ for $X_{PG} = 0.75$. The thick solid lines refer to scenario A (see text). It assumes a "sudden" internalization threshold, $(P/L)^{threshold} = (P/L)_I$, at which the bilayers become completely permeable and, consequently, γ turns from γ_I to γ_{II}. The curve below corresponds to a gradual internalization process according to scenario B. Here, only penetratin molecules exceeding a certain local threshold concentration of bound peptide, can actually permeate the bilayer.

peptide can actually permeate the bilayer as suggested by case B (Fig. 7).

Internalization is triggered by a subtle interplay between the anionic surface charge density and the effective cationic charge of the peptide.[17] The minimum fraction of DOPG to induce internalization is about 50% of the total lipid content. At the higher content of anionic peptide, $X_{PG} = 0.75$, the permeabilization threshold is reached before the outer vesicle surfaces saturate with bound peptide (Fig. 7). The q_P courses at $X_{PG} = 0.5$ can be qualitatively understood if the system reaches the threshold just only in the saturation range III. The absolute q_P values show a local minimum followed by a maximum in the in the range of its sigmoidal decrease (Fig. 7). In addition, the calorimetric traces broaden in the same P/L range (see ref. 17). Both effects are characteristic signatures of a peptide internalization. Internalization is obviously paralleled by saturation. The respective theoretical curve for range II ($X_{PG} = 0.5$) are calculated using an intermediate accessibility factor $\gamma = 0.7$. It can be explained by "partial" internalization, if peptide binding virtually stops in the range of progressive internalization due to saturation. We suggest that the bilayer becomes impermeable before penetratin completely equilibrates between the inner and outer vesicle surfaces. Alternatively, also slow kinetics of internalization at these conditions can mask complete equilibration in the ITC experiment (*vide infra*).

The measured cumulative heat over range II at $X_{PG} = 0.75$ roughly agrees with that of the two considered models. Hence, our data provide no indication of a significant enthalpic contribution originating from the internalization process. The ITC calorimeter measures reactions with a characteristic time constant ranging from seconds up to several tens of minutes. Slower processes are hardly detected. Fluorescently labeled penetratin was shown to transverse lipid membranes in minutes up to hours.[8,15] This time is equal to or longer than the characteristic time of the ITC experiment. Therefore, we cannot exclude that internalization events were only incompletely detected by the calorimetric method.

Summary and conclusions

We studied the thermodynamics of binding of the cell-penetrating peptide penetratin with lipid membranes as a function of the content of anionic lipid by means of isothermal titration calorimetry. So-called lipid-to-peptide and peptide-to-lipid titration experiments were performed. They provide estimations of the differential binding enthalpy at high and low peptide concentrations, respectively. The experimental data were interpreted in terms of the surface partitioning model which assumes that electrostatic interactions cause an enrichment of cationic peptide in the aqueous phase near the anioinic membrane interface.

The binding of the peptide to the lipid bilayer is accompanied by an enthalpy gain of about $-(20–30)$ kJ mol^{-1}. This value roughly agrees with the gain of Gibbs free energy upon binding. Consequently, the association of penetratin with lipid bilayers is essentially driven by enthalpy. Recently published data[11,14] let us suggest that the enthalpic gain results from the non-classical hydrophobic effect (*i.e.* specific interactions between the lipid and the peptide and/or a strengthening of lipid–lipid interactions) and a membrane-induced conformational change of penetratin from a random coil into an α-helical and/or β-sheet structure. Subtle alterations of the differential binding enthalpy as a function of the content of anionic lipid of the membrane and of the molar ratio bound peptide-to-lipid probably reflect variations of the secondary structure of bound penetratin. The small entropic contribution is compatible with a superficial binding mode of the peptide which only weakly perturbs the membrane.

The vesicle membranes become permeable at a molar ratio peptide-to-lipid exceeding a threshold value which is characterized by a local minimum of the exothermic reaction heat in the respective P-to-L titration experiments. The enthalpic effect can be qualitatively explained in terms of simple scenarios which assume either complete or partial equilibration of penetratin concentration through the bilayer membranes.

The change of secondary structure upon membrane binding and specific peptide–lipid interactions. possibly affect the potency of Trojan peptides to permeate the lipid bilayer. Our subsequent study will be aimed to elucidate molecular details of peptide-lipid interactions and the conformation and orientation of membrane bound penetratin peptide.

References

1 A. Prochiantz, *Curr. Opin. Neurobiol.*, 1996, **6**, 629–634.
2 M. Pooga, U. Soomets, M. Hällbrink, A. Valkna, K. Saar, K. Rezai, U. Kahl, J. Hao, X. Xu, Z. Wiesenfeld-Hallin, T. Hokfelt, T. Bartfai and U. Langel, *Nat. Biotechnol.*, 1998, **16**, 857–861.
3 D. J. Mitchell, D. T. Kim, L. Steinman, C. G. Fathman and J. B. Rothbard, *J. Pept. Res.*, 2000, **56**, 318–325.
4 J. B. Rothbard, S. Garlington, Q. Lin, T. Kirschberg, E. Kreider, P. L. McGrane, P. A. Wender and P. A. Khavari, *Nature Med.*, 2000, **6**, 1253–1257.
5 J. B. Rothbard, E. Kreider, C. L. Van Deusen, L. Wright., B. L. Wylie and P. A. Wender, *J. Med. Chem.*, 2002, **45**, 3612–3618.
6 G. Drin, H. Demene, J. Temsamani and R. Brasseur, *Biochemistry*, 2001, **40**, 1824–1834.
7 D. Derossi, A. H. Joliot, G. Chassaing and A. Prochiantz, *J. Biol. Chem.*, 1994, **269**, 10444–10450.
8 P. E. G. Thoren, D. Persson, M. Karlsson and B. Norden, *FEBS Lett.*, 2000, **482**, 265–268.
9 D. Persson, P. E. G. Thoren and B. Norden, *FEBS Lett.*, 2001, **505**, 307–312.
10 D. Persson, P. E. G. Thoren, M. Herner, P. Lincoln and B. Norden, *Biochemistry*, 2003, **42**, 421–429.
11 Z. Salamon, G. Lindblom and G. Tollin, *Biophys. J.*, 2003, **84**, 1796–1807.
12 B. Christiaens, S. Symoens, S. Vanderheyden, Y. Engelborghs, A. Joliot, A. Prochiantz, J. Vanderkerckhove, M. Rosseneu and B. Vanloo, *Eur. J. Biochem.*, 2002, **269**, 2918–2926.
13 M. Lindgren, X. Gallet, U. Soomets, M. Hällbrink, E. Brakenhielm, M. Pooga, R. Brasseur and U. Langel, *Bioconjugate Chem.*, 2000, **11**, 619–626.
14 M. Magzoub, L. E. Erikson and A. Gräslund, *Biochim. Biophys. Acta*, 2002, **1563**, 53–63.
15 M. Hällbrink, A. Floren, A. Eomquist, M. Pooga, T. Bartfai and Ü. Langel, *Biochim. Biophys. Acta*, 2001, **1515**, 101–109.
16 J. Seelig, *Biochim. Biophys. Acta*, 1997, **1331**, 103–116.
17 H. Binder and G. Lindblom, *Biophys. J.*, 2003, **85**, 982–995.
18 G. Beschiaschvili and J. Seelig, *Biochemistry*, 1990, **29**, 10995–11000.
19 S. H. White, W. C. Wimley, A. S. Ladokhin and K. Hristova, *Methods Enzymol.*, 1998, **295**, 62–87.
20 M. Eisenberg, T. Gresalfi, T. Riccio and S. McLaughlin, *Biochemistry*, 1979, **18**, 5213–5223.
21 M. Langner and K. Kubica, *Chem. Phys. Lipids*, 1999, **101**, 3–35.
22 T. E. Thorgeirsson, Y. G. Yu and Y. K. Shin, *Biochemistry*, 1995, **34**, 5518–5552.
23 A. Lau, A. McLaughlin and S. McLaughlin, *Biochim. Biophys. Acta*, 1981, **645**, 279–292.
24 M. R. Wenk and J. Seelig, *Biochemistry*, 1998, **37**, 3909–3916.
25 T. Wieprecht, O. Apostolov, M. Beyermann and J. Seelig, *J. Mol. Biol.*, 1999, **294**, 785–794.
26 T. Wieprecht, O. Apostolov, M. Beyermann and J. Seelig, *Biochemistry*, 2000, **39**, 442–452.
27 A. S. Ladokhin and S. H. White, *J. Mol. Biol.*, 2001, **309**, 543–552.
28 T. Wieprecht, M. Beyermann and J. Seelig, *Biochemistry*, 1999, **38**, 10377–10387.
29 C. Tanford, *The Hydrophobic Effect*, Wiley and Sons, New York, 1973.

30 S. J. Gill and I. Wadsö, *Proc. Natl. Acad. Sci. USA*, 1976, **73**, 2955–2958.

31 S. H. White and W. C. Wimley, *Biochim. Biophys. Acta*, 1998, **1376**, 339–352.

32 E. Bellet-Amalric, D. Blaudez, B. Desbat, F. Graner, F. Gauthier and A. Renault, *Biochim. Biophys. Acta*, 2000, **1467**, 131–143.

33 H. Binder and G. Lindblom, *Biophys. J.*, 2003, submitted.

34 M. Magzoub, K. Kilk, L. E. Erikson, Ü. Langel and A. Gräslund, *Biochim. Biophys. Acta*, 2001, **1512**, 77–89.

35 A. A. Yaroslavov, O. Y. Kuchenkova, I. B. Okuneva, N. S. Melik-Nubarov, N. O. Kozlova, V. I. Lobyshev, F. M. Menger and V. A. Kabanov, *Biochim. Biophys. Acta*, 2003, **1611**, 44–54.

36 H. H. Heerklotz, *Biophys. J.*, 2001, **81**, 184–195.

37 H. Heerklotz and J. Seelig, *Biochim. Biophys. Acta*, 2000, **1508**, 69–85.